CHAPTER VII

PREFERENTIAL OXIDATION (PROX) OF CO IN H_2-RICH GAS USING Pt/MESOPOROUS $AlPO_4$-5 AND SAPO-5 CATALYSTS PREPARED FROM ATRANE PRECURSORS VIA MICROWAVE HEATING

7.1 Abstract

Pt loaded mesoporous $AlPO_4$-5 and SAPO-5 catalysts were prepared using alumatrane and silatrane as aluminum and silica sources, respectively, under microwave heating. Triethylamine (TEA) was used as a structure-directing agent. The samples were characterized by x-ray diffractomerter (XRD), scanning electron microscope (SEM), transmission electron microscope (TEM), and surface area measurement. The activity test was carried out on the preferential oxidation (PROX) of CO in H_2-rich over the temperature range of 80 °–300 °C. As increasing Pt content, the activity was also increased. The catalytic activity of Pt impregnated mesoporous $AlPO_4$-5 was the best, comparing to Pt impregnated $AlPO_4$-5 synthesized using commercial aluminum and Pt-$AlPO_4$-5 prepared via the sol-gel process.

7.2 Introduction

$AlPO_4$-5 zeotype with AFI type, first published in 1982 [1], composed of one-dimensional channels formed by 12-membered rings channels parallel to the *c*-axis with a pore diameter in micropore region of 0.73 nm. The substitution of Si into the $AlPO_4$-5 framework generated SAPO-5. The framework of SAPO-5 zeotype is also similar to that of $AlPO_4$-5 with AFI structure. AFI type has attracted much attention as a result of zeolitic properties, excellent thermal stability, use in catalysis

reactions, and potential applications, such as host matrix to organize dye molecules for nonlinear optics [2]. Both $AlPO_4$-5 and SAPO-5 prepared under microwave heating showed superior properties, as compared to materials obtained from conventional heating, viz. using shorter reaction time, uniforms crystal size distribution [3], higher phase purity [4], and phase selective crystallization by getting rid of unstable materials [5].

Wongkasemjit and coworkers have been synthesized many metal alkoxide precursors, e.g. alumatrane [6] and silatrane [7], via the "Oxide One Pot Synthesis (OOPS)" process. This reaction gives highly pure and moisture stable metal alkoxides that have been successfully applied as precursors for synthesizing various zeolites, such as MFI [8], K-H [9], and MCM-41 [10]. Recently, a new family of crystalline zeolitic materials, mesoporous zeolite single crystals, was reported to overcome a problem of diffusion limitation of micropore zeolites [11–13]. The mesopore improves the mass transfer to and from the active sites. These mesoporous zeolites are found to enhance catalytic properties, as compared to conventional zeolites.

Pt loaded $AlPO_4$-5 and SAPO-5 catalysts were prepared to test activity performance on isomerization of hydrocarbon [14–17]. Pt metal, generally on alumina support, has been widely used on the PROX of CO reaction [18–20] because of its high resistance to deactivation by CO_2 or H_2O [21]. The PROX of CO unit is needed for polymer electrolyte membrane fuel cells (PEMFC). Since H_2, used as fuel in PEMFC and obtained from the reforming of hydrocarbon fuel, contained the upper limitation of CO level, the CO concentration has to be reduced to lower than 10 ppm for protecting platinum electrodes in PEMFC. The use of zeolites as support for Pt based catalysts were applied by many groups [22-24] to increase selectivity and chemisorption of reactant in the pore, comparing Al_2O_3 support. Pt/A zeolite showed a maximum CO conversion at 250 °C [22]. Igarashi *et al.* [23] revealed that Pt supported zeolite A, zeolite X and MOR on the PROX of CO did not give the achievement of 100 % CO conversion at 1 % O_2 in gas mixture. A higher content of O_2 needed to reach complete CO conversion [23], however, an explosion is risk. The kinetics of CO oxidation in H_2-rich on Pt/MOR and Pt/Al_2O_3 was evaluated [25].

Pt/MOR illustrated a wider operation temperature range than Pt/Al_2O_3. Sebastian *et al.* [26] also investigated on Pt supported zeolites (MOR, ZSM-5, FAU and ETS-10), and found that Pt/FAU was the only one material attained 100 % CO conversion due to its larger pore size and higher dispersion of Pt.

The aim of this work is thus to load Pt metal onto mesoporous $AlPO_4$-5 and SAPO-5 synthesized from atrane precursors via microwave technique using triethylamine (TEA) as a structure-directing agent. These catalysts are investigated the efficiency on the preferential oxidation (PROX) of CO in H_2-rich gas.

7.3 Experimental

7.3.1 Precursor Synthesis

Alumatrane, used as the alumina source, was synthesized, following the method in reference 6. Aluminum hydroxide (0.1 mol, Sigma Chemical Co.), triisopropanolamine (TIS, 0.125 mol, Aldrich Chemical Co. Inc., USA), and ethylene glycol (EG, 100 mL, J.T. Baker, Inc., Phillipsburg, USA) were homogeneously mixed at room temperature. The mixture was then heated to 200 °C under nitrogen in an oil bath for 10 h. Excess EG was eliminated under vacuum (10^{-2} Torr) at 110 °C. The crude product was washed with acetonitrile (Lab-Scan Company Co., Ltd.) and dried under vacuum at room temperature. Dried products were characterized using Thermogravimetric analysis (TGA) and Fourier transform infrared spectroscopy (FTIR).

FTIR: 3700–3300 cm^{-1} (ν OH), 2750–3000 cm^{-1} (ν CH), 1650 cm^{-1} (ν OH overtone), 1460 cm^{-1} (δ CH), 1078 cm^{-1} (ν Al–O–C) and 500–800 cm^{-1} (ν Al–O). TGA: 33 % char yield which is larger than the theoretical ceramic value of 23.7 %. This may be due to the incomplete combustion which was confirmed by the black color of the char.

In case of silatrane used as the silica source, the synthesis followed the method reported in reference 7. Fumed silica and triethanolamine were used instead of aluminum hydroxide and TIS.

FTIR: 3700–3300 cm^{-1} (ν OH), 2800–3000 cm^{-1} (ν CH), 1244–1275 cm^{-1} (ν CN), 1170–1117 cm^{-1} (ν Si–O), 1093 cm^{-1} (ν Si–O–C), 1073 cm^{-1} (ν CO), 785 and 729 cm^{-1} (Si–O–C), and 579 cm^{-1} (ν N → Si). TGA: 19 % ceramic yield which was close to the theoretical value, 18.5 %.

7.3.2 Catalyst Preparation

The synthesis of mesoporous $AlPO_4$-5 and SAPO-5 zeotype followed the procedure reported in references 27 and 28, respectively. The reagents employed were alumatrane, silatrane, phosphoric acid (Merck, 85 %), TEA (Fisher Scientific). A synthesis mixture was hydrothermally crystallized using microwave technique. The products were filtered, washed, and dried. The as-synthesized products were calcined at 600 °C for 7 h. In case of $AlPO_4$-5 zeotype using commercial aluminum source, aluminum isopropoxide (Aldrich Chemical Co. Inc., USA) was used.

The impregnation method was used to prepare catalysts. $(NH_3)_4PtCl_2$ [Alfar Aesar], used as a platinum source, was dissolved in distilled water before adding $AlPO_4$-5/SAPO-5 with stirring. The catalysts were dried at 110 °C overnight and subsequently calcined at 500 °C for 4 h. The amount of $(NH_3)_4PtCl_2$ used was varied (1, 3 and 5 % w/w). For the synthesis via the sol-gel method, $(NH_3)_4PtCl_2$ was mixed with alumatrane, silatrane, and phosphoric acid before adding TEA.

7.3.3 Catalyst Characterization

Functional groups of materials were identified by FTIR (Nicolet, NEXUS 670) with a resolution of 4 cm^{-1}. TGA was performed on Pyris Diamond Perkin Elmer TG-DTA with a heating rate of 10 °C/min in a range of room temperature to 750 °C under nitrogen atmosphere to determine the thermal stability. BET surface area measurement, pore volume, and pore size distribution were evaluated using nitrogen at 77 K in an Autusorb-1 gas sorption system (Quantasorb JR). Samples were degassed at 250 °C under a reduced pressure prior to each measurement. The metal distributions were observed using TEM (JEOL JEM-2100). Calcination was carried out on a Carbolite Furnace (CFS 1200) with a heating rate of 1 °C/min. Microwave heating technique was carried out on Milestone's Ethos microwave solvent extraction labstation with the frequency of the microwave radiation of 2.45 GHz for hydrothermal crystallization. The crystalline phases were determined using a Rigaku XRD equipped with a RINT 2200 wide angle goniometer, using CuKα radiation (1.5406 Å) with a voltage of 40 KV and a current of 30 mA. CO chemisorption was conducted to determine Pt dispersion. Prior to pulse chemisorption, all samples were purged in purified He at 110 °C for 30 min and then cooled to 50 °C in He atmosphere. The chemisorption of CO was measured by using a thermal conductivity detector (TCD).

7.3.4 Catalyst Testing

Catalytic activity was carried out on the PROX of CO reaction. A 0.1 g of catalyst was loaded in a U-tube micro-reactor covered with quartz wool. The catalytic activity was investigated in the temperature range of 80 °-300 °C. Gas compositions consisting of 1 % CO, 1 % O_2, 40 % H_2, and He balance were controlled using mass flow controllers with a total flow rate of 50 ml/min. The products were measured by gas chromatography (Agilent Technologies 6890N GC) equipped with a thermal conductivity detector (TCD) to analyze the concentration of H_2, CO, O_2, and CO_2. The CO and O_2 conversions were determined, based on the CO and O_2 consumption in % volume, respectively, during carry out the PROX reaction.

The selectivity of CO was formulated by the O_2 used for CO oxidation directly divided by the total O_2 reacted in % volume.

7.4 Results and Discussion

7.4.1 Catalyst Characterization

Pt metal was attributed to mesoporous $AlPO_4$-5 and SAPO-5 synthesized from alumatrane and silatrane via microwave heating. SEM micrographs showing morphologies of Pt impregnated mesoporous $AlPO_4$-5 (Pt/$AlPO_4$-5, Figure 7.1a), and mesoporous SAPO-5 (Pt/SAPO-5, Figure 7.1b) materials revealed that modification of $AlPO_4$-5 and SAPO-5 by Pt impregnation did not affect on the morphology of these materials. Nevertheless, Pt/$AlPO_4$-5 still maintained a long rod-like shape as found in reference 27. Pt/SAPO-5 also had plate-like as seen in reference 28. However, Pt loaded $AlPO_4$-5 prepared by the sol-gel process (Pt-$AlPO_4$-5), as shown in Figure 7.1c, exhibited a shingle-like shape with sharpening at both ends. Pt metal hindered the formation of metal oxide network with AFI structure and the crystal growth. This shape was also observed by the work done by Iwasaki *et al.* [29], who synthesized $AlPO_4$-5 zeotype, due to the immature growth of crystals or polarization effect of the non-symmetric structure caused by alternating of Al and P atoms in $AlPO_4$-5 framework.

XRD in Figure 7.2 was carried out to characterize the incorporation of Pt metal on mesoporous $AlPO_4$-5 and SAPO-5 and showed the presence of Pt metal at 2Θ values of 39.8 ° (Pt{111}) and 46.3 °, as denoted in references 30 and 31. The intensity of the Pt peak increases with the Pt content. A similar trend was also observed to the SAPO-5 (Figure 7.3). Pt particle sizes for all samples, calculated from the full width half maximum (FWHM) of the main peak at 2Θ equal to 39.8 ° according to Scherrer's equation, were in the range of 12–17 nm. TEM result shows

well dispersion of Pt particles on mesoporous $AlPO_4$-5 support prepared by the impregnation method (Figure 7.4). The function of the preparation method was observed in Figure 7.5. The relative intensity of the Pt prepared by the sol-gel process (Figure 7.5c) is lower than that synthesized by the impregnation method (Figure 7.5a). This may be due to less Pt participating in the sol-gel process or some Pt particles were loss during the synthesis. Table 7.1 summarizes the BET surface area before and after Pt loading. The BET surface area decreased after metal loading because the pores were blocked by Pt metal, as also observed by Padilla *et al.* [21].

7.4.2 Activity testing

The PROX of CO reaction in H_2-rich gas with a gas mixture of 1 % CO, 1 % O_2, 40 % H_2 was carried out to study the catalytic performance of Pt loaded mesoporous $AlPO_4$-5 and SAPO-5 with AFI type. The effect of % w/w Pt content on $AlPO_4$-5 over the PROX of CO reaction was investigated in Figure 7.6 exhibiting CO conversion (%), O_2 conversion (%) and, CO selectivity (%) as a function of reaction temperature. Kotobuki *et al.* [32] reported that Pt particles had a function of adsorption sites for CO and H_2. The CO molecules were strongly absorbed on Pt particles at low temperature [20], causing low % CO conversion. The CO and O_2 conversions began to increase as the temperature was increased up to 160 °C, and then, rapidly increased as increasing reaction temperature owing to CO molecules partially desorbed [20]. The 1 % w/w Pt/$AlPO_4$-5 showed an approximately 70 % CO conversion at the reaction temperature of 260 ° to 300 °C. A 100 % CO conversion was reached for the sample prepared with high Pt content of 3% and 5% w/w at the reaction temperatures of 220 ° and 240 °C, respectively. As compared to the work done by Igarashi *et al.* [23], Pt impregnated with 6 % w/w on zeolite supported catalysts in a 1 % O_2 mixed gas was not enough for oxidation of CO to obtain 100% CO conversion. They needed more amount of O_2 to reach complete conversion, e.g. 2 % O_2 using Pt supported zeolite A and zeolite X, and 1.5 % for Pt supported mordernite [23]. Above the reaction temperature of 260 °C in our case, the

CO conversion tended to slightly decrease due to the competition of H_2 oxidation reaction [23] or reverse water gas shift (RWGS) to form CO [26, 31]. This reaction prefers to take place at high operating temperature, influencing on a slight decrease in CO selectivity as well. However, the O_2 conversion still sustained 100 % conversion due to the oxygen needed for H_2 oxidation. Although, the catalysts showed active performance at high reaction temperature, it is not disadvantage due to the fact that the PROX unit is set up between the low temperature WGSR (200 °-300 °C) and the PEMFC (80 °-100 °C), the effective catalyst should be operated between these temperatures [33]. Thus, Pt/$AlPO_4$-5 can be used as a catalyst for the PROX of CO without adjusting temperature before feeding to the system. Besides, the catalysts also achieved a complete CO removal in a wider operation temperature. Similar trend was also observed for Pt/SAPO-5 as a function of reaction temperature (Figure 7.7). However, in this case, only 5% w/w Pt loading could achieve 100% CO conversion. CO chemisorption isotherms (Figure 7.8) determined Pt dispersion on 3% Pt/mesoporous $AlPO_4$-5 and 3% Pt/mesoporous SAPO-5. The result showed Pt dispersion value of 56.2% and 30.1%, respectively, causing Pt supported on mesoporous $AlPO_4$-5 enhanced PROX of CO activity due to it showed higher Pt dispersion than Pt supported on mesoporous SAPO-5.

The roles of the method used for loading Pt and the aluminum precursor used were also investigated on the PROX of CO (Figure 7.9). The comparison of the impregnation method and the sol-gel process was evaluated. Surprisingly, the impregnation method enhanced better activity than the sol-gel process. As discussed above, some Pt particles may be loss during the sol-gel processing, causing less Pt present in the catalyst and as a result giving lower performance, as compared to the sample prepared via the impregnation method. This finding was also observed by Luengnaruemitchai's work on Pt/LTA zeolite [24]. The advantage of Pt impregnated on mesoporous $AlPO_4$-5 using atrane precursor, as compared to $AlPO_4$-5 using commercial aluminum is shown in Figure 7.9. It seems difficult to obtain 100% CO conversion even at high temperature for the Pt impregnated $AlPO_4$-5 prepared using commercial aluminum. On the contrary, the complete removal of CO was obtained on Pt impregnated on mesoporous $AlPO_4$-5 using atrane precursor. This may be due

to the pore volume of the mesopores calculated according to the BJH method (desorption) of the $AlPO_4$-5 zeotype prepared using atrane precursor contained more mesopores volume (0.075 cc/g) than that observed from $AlPO_4$-5 synthesized using commercial aluminum (0.017 cc/g). As verified by Xiao *et al.* [34], the presence of mesopore in Beta zeolite exhibited a higher activity and selectivity, as compared to conventional Beta zeolite on the alkylation of benzene with propan-2-ol because the mesopores enhanced the mass transport of the reactants and products, and overcame diffusion limitation of the micropores in zeolite.

7.5 Conclusions

Pt impregnated mesoporous $AlPO_4$-5 and SAPO-5 catalysts synthesized from atrane precursors under microwave radiation using TEA as structure-directing agent was investigated the activity on the PROX of CO. A higher impregnated Pt enhanced the catalytic activity for both supports. A better catalytic performance was achieved for the complete CO removal on Pt impregnated mesoporous $AlPO_4$-5 than those prepared via the sol-gel process or Pt impregnated on $AlPO_4$-5 zeotype using commercial aluminum.

7.6 Acknowledgements

This research work is financially supported by the Postgraduate Education and Research Program in Petroleum and Petrochemical Technology (ADB) Fund, Thailand, the Ratchadapisake Sompote Fund, Chulalongkorn University, and the Development and Promotion of Science and Technology Thailand Project (DPST). The authors would like to express their sincere appreciation to Assistant Professor Apanee Luengnaruemitrchai and Dr. Pattarasuda Naknam for their assistance in the use of the PROX unit.

7.6 References

1. S.T. Wilson, B.M. Lok, C.A. Messina, T.R. Cannan, E.M. Flanigen, J. Am. Chem. Soc. 104 (1982) 1146.
2. J. Caro, G. Finger, J. Kornatowski, J. Richter-Mendau, L. Werner, B. Zibrowius, Adv. Mater. 4 (1992) 273.
3. T. Kodaira, K. Miyazawa, T. Ikeda, Y. Kiyozumi, Micropor. Mesopor. Mater., 29 (1999) 329.
4. S. Mintova, S. Mo, T. Bein, Chem. Mater. 10 (1998) 4030.
5. J.W. Yoon, S.H. Jhung, Y.H. Kim, S.E. Park, J.S. Chang, Bull. Korean Chem.Soc. 26 (2005) 558.
6. Y. Opornsawad, B. Ksapabutr, S. Wongkasemjit, R.M. Laine, J. Eur. Polym. 37 (2001) 1877.
7. P. Piboonchaisit, S. Wongkasemjit, R. Lanine, ScienceAsia. 25 (1999) 113.
8. P. Phiriyawirut, R. Magaraphan, A.M. Jamieson, S. Wongkasemjit, Micropor. Mesopor. Mater. 64 (2003) 83.
9. M. Sathupunya, E. Gulari, A. Jamieson, S. Wongkasemjit, Micropor. Mesopor. Mater. 69 (2004) 157.
10. N. Thanabodeekij, S. Sadthayanon, E. Gulari, S. Wongkasemjit, Mater. Chem. Phys. 98 (2006) 131.
11. C.J.H. Jacobsen, C. Madsen, J. Houzvicka, I. Schmidt, A. Carlsson, J. Am. Chem. Soc. 122 (2000) 7116.
12. V. Naydenov, L. Tosheva, O.N. Antzutkin, J. Sterte, Micropor. Mesopor. Mater. 78 (2005) 181.
13. K. Egeblad, M. Kustova, S.K. Klitgaard, K. Zhu, C.H. Christensen, Micropor. Mesopor. Mater. 101 (2007) 214.

14. J.H., Zhu, J.L., Dong, Q.H., Xu, React. Kin. and Catal. Lett. 60 (1997) 113.

15. T.C. Xiao, H.T. Wang, Y.L. Lu, L.D. An, H.L. Wang, Korean J. Chem. Eng. 15 (1998) 505.

16. N. Kumar, J.I. Villegas, T. Salmi, D.Y., Murzin, T. Heikkila, Catal. Today. 100 (2005) 355.

17. R. Roldan, M. Sanchez-Sanchez, G. Sankar, F.J. Romero-Salguero, C. Jimenez-Sanchidrian, Micropor. Mesopor. Mater. 99 (2007) 288.

18. M.J. Kahlich, H.A. Gasteiger, R.J. Behm, J. Catal. 171 (1997) 93.

19. D.H. Kim, M.S. Lim, Appl. Catal. A: Gen., 224, (2002) 27.

20. A. Manasilp, E. Gulari, Appl. Catal. B: Envi. 37 (2002) 17.

21. R. Padilla, M. Benito, L. Rodriguez, A. Serrano-Lotina, L. Daza, J. Power Sources. 192 (2009) 114.

22. M. Watanabe, H. Uchida, H. Igarashi, M. Suzuki, Chem. Lett. (1995) 21.

23. H. Igarashi, H. Uchida, Y. Suzuki, M. Watanabe, Appl. Catal. A: Gen. 159 (1997) 159.

24. A. Luengnarumitchai, M. Nimsuk, P. Naknam, S. Wongkasemjit, S. Osuwan, Int. J. Hydrogen Energy. 33 (2008) 206.

25. S. Ren, X. Hong, Fuel Process Technol. 88 (2007) 383.

26. V. Sebastian, S. Irusta, R. Mallada, J. Santamaria, Appl. Catal. A: Gen. 366 (2009) 242.

27. K. Utchariyajit, S. Wongasemjit, Micropor. Mesopor. Mater. 114 (2008) 175.

28. K. Utchariyajit, S. Wongkasemjit, "Effect of synthesis parameters on mesoporous SAPO-5 with AFI-type formation via microwave radiation using alumatrane and silatrane precursors", Micropor. Mesopor. Mater, accepted manuscript.

29. A. Iwasaki, T. Sano, T. Kodaira, Y. Kiyozumi, Micropor. Mesopor. Mater. 64 (2003) 145.

30. J.L. Ayastuy, A. Gil-Rodriguez, M.P. Gonzalez-Marcos, M.A. Gutierrez-OrtiZ, Int.J. Hydrogen Energy 31 (2006) 2231.

31. I. Rosso, C. Galletti, S. Fiorot, G. Saracco, E. Garrone, V. SpecchiaJ. Porous. Mater. 14 (2007) 245.

32. M. Kotobuki, A. Watanabe, H. Uchida, H. Yamashita, M. Watanabe, J. catal. 236 (2005) 262.

33. S. Huang, K. Hara, A. Fukuoka, Energy Environ. Sci. 2 (2009) 1060.

34. F.S. Xiao, L. Wang, C. Yin, K. Lin, Y. Di, J. Li, R. Xu, D.S. Su, R. Schlogl, T. Yokoi, T. tatsumi, Angew. Chem. Int. Ed. 45 (2006) 3090.

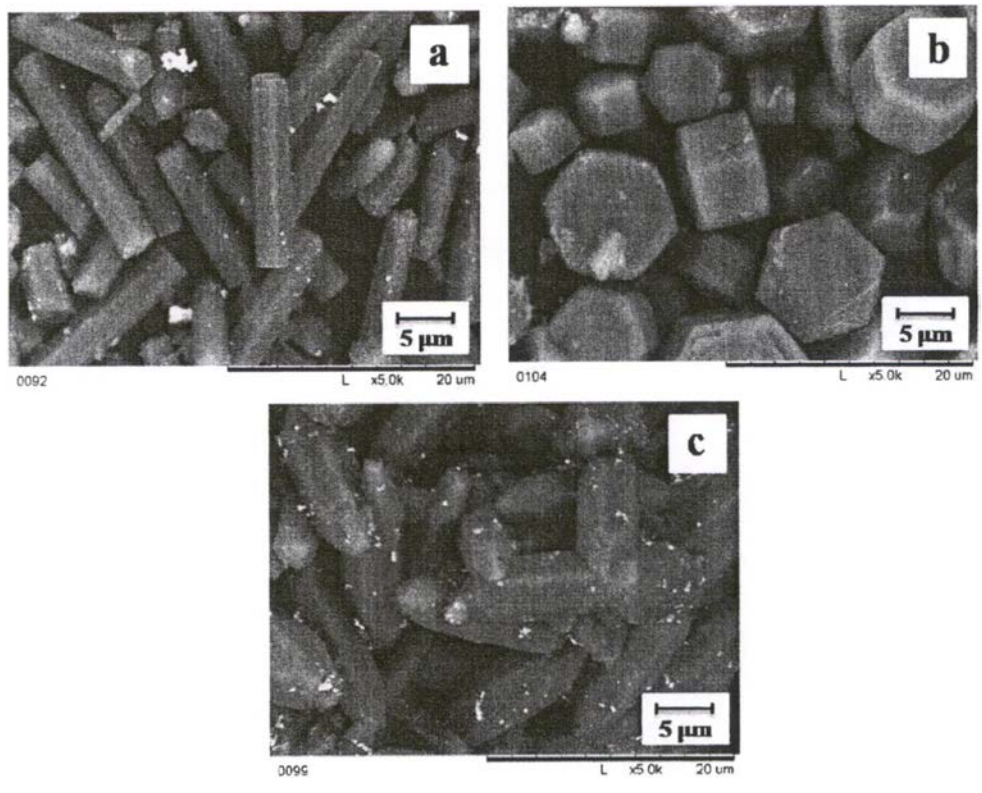

Figure 7.1 SEM micrographs of Pt impregnated on (a) $AlPO_4$-5 and (b) SAPO-5 using atrane precursors, and (c) Pt prepared via the sol-gel process.

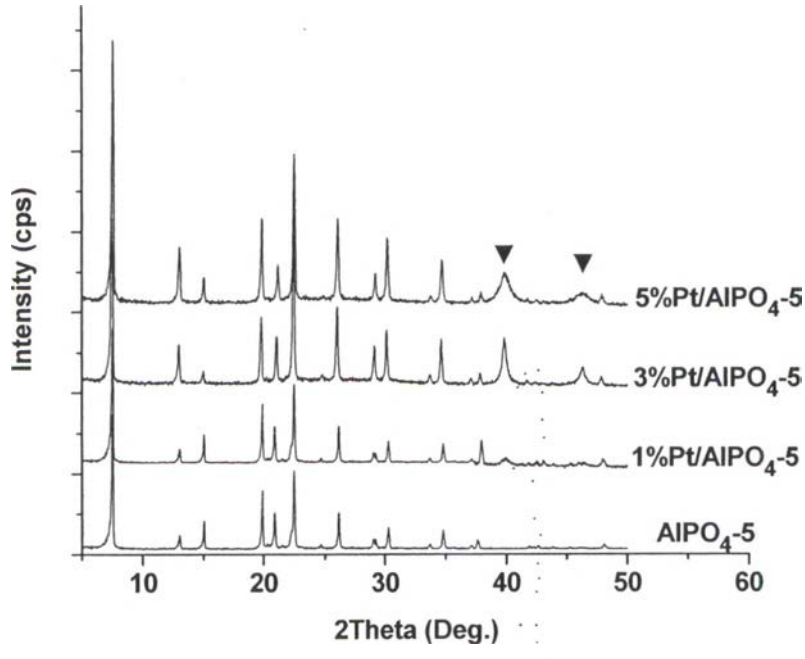

Figure 7.2 XRD patterns of Pt impregnated $AlPO_4$-5 using atrane precursor at various % w/w Pt contents (▼ peaks of metallic platinum).

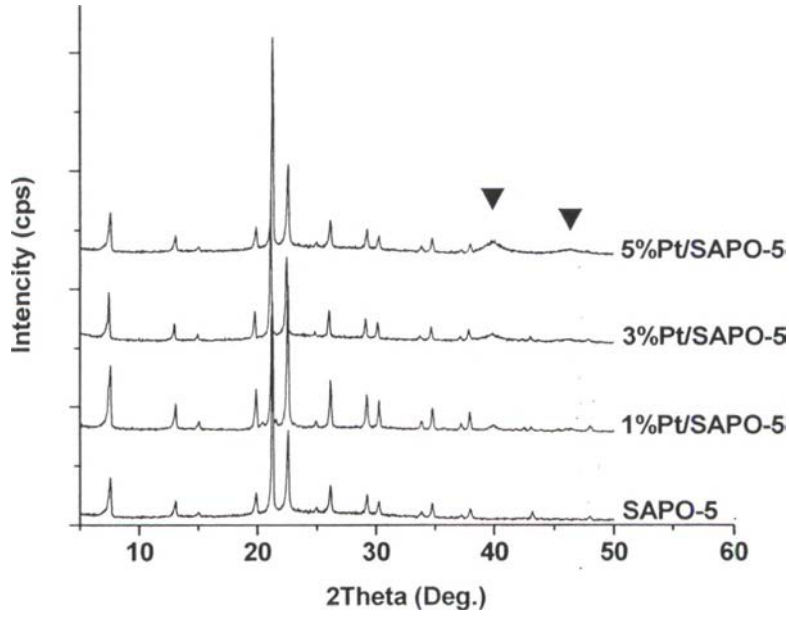

Figure 7.3 XRD patterns of Pt impregnated on SAPO-5 using atrane precursors at various % w/w Pt contents (▼= peaks of metallic platinum).

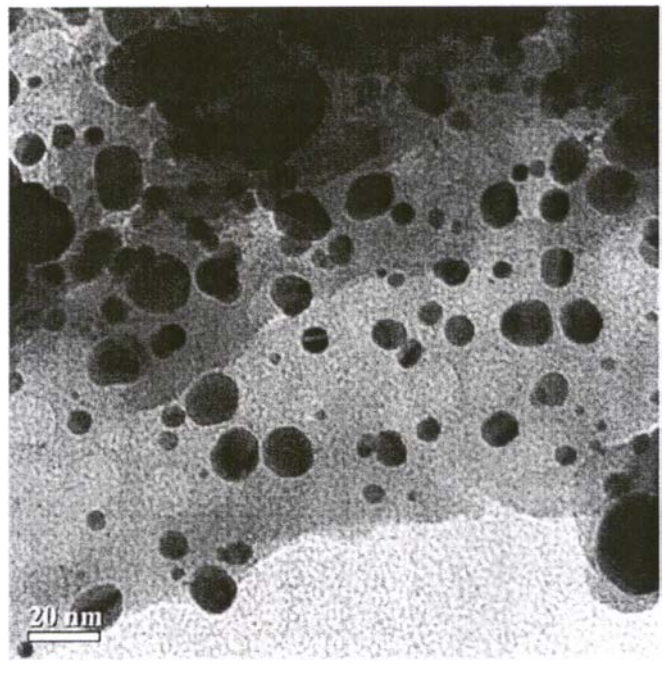

Figure 7.4 TEM micrograph of 3 % Pt impregnated on $AlPO_4$-5

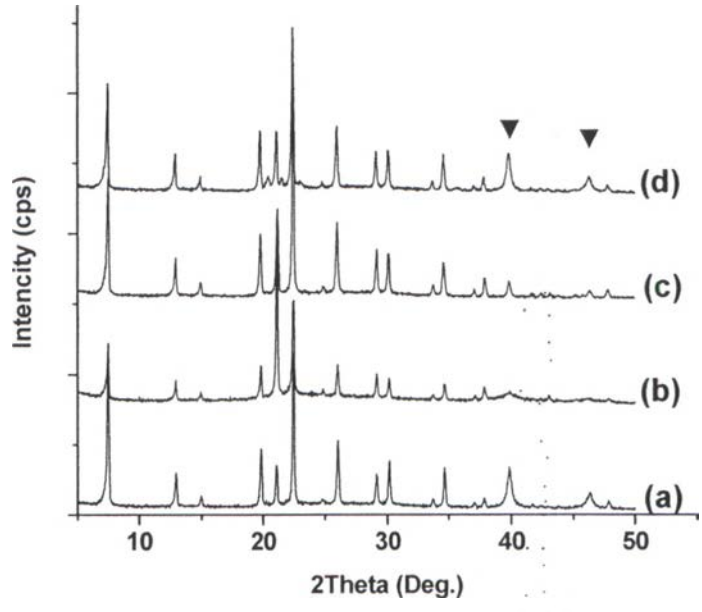

Figure 7.5 XRD patterns of Pt impregnated on (a) $AlPO_4$-5 and (b) SAPO-5 using atrane precursors, (c) Pt loaded via the sol-gel process on $AlPO_4$-5 using atrane precursor, and (d) Pt impregnated on $AlPO_4$-5 using aluminum isopropoxide precursor at 3% w/w Pt content (▼ = peaks of metallic platinum)

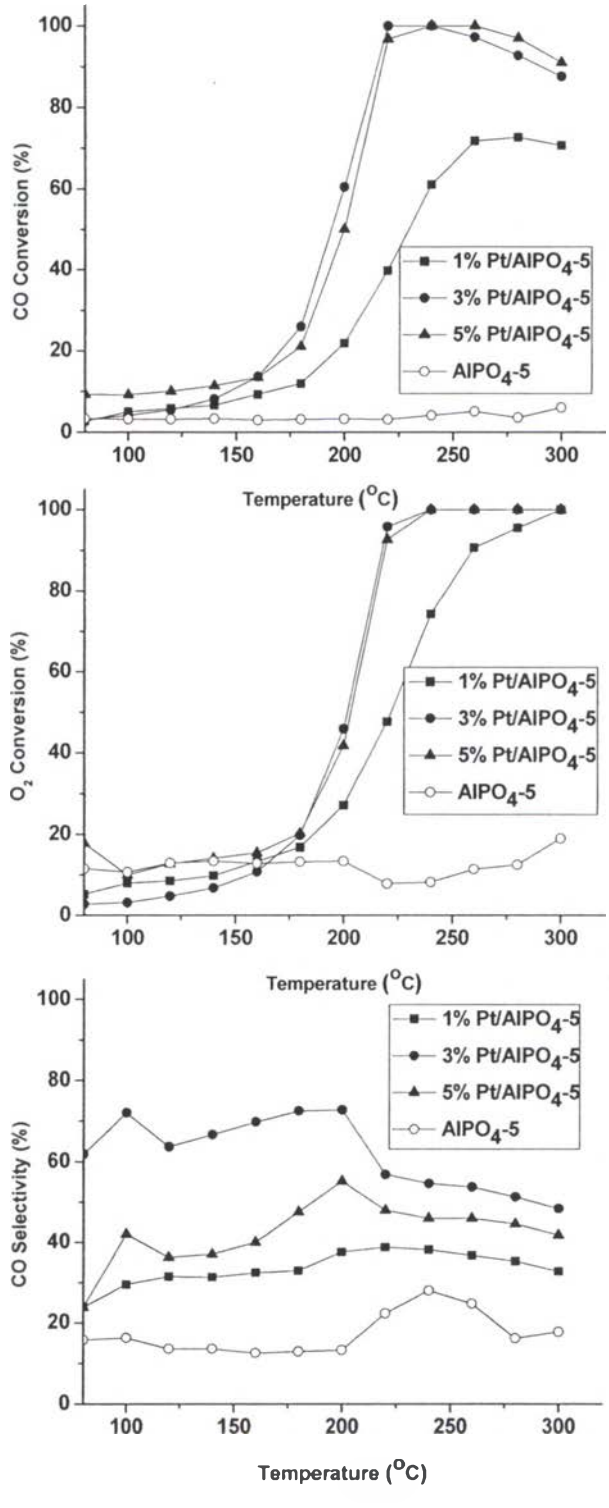

Figure 7.6 CO Conversion (%), O_2 Conversion (%), and CO Selectivity (%) of Pt impregnated on $AlPO_4$-5 prepared using atrane precursors at various % w/w Pt contents.

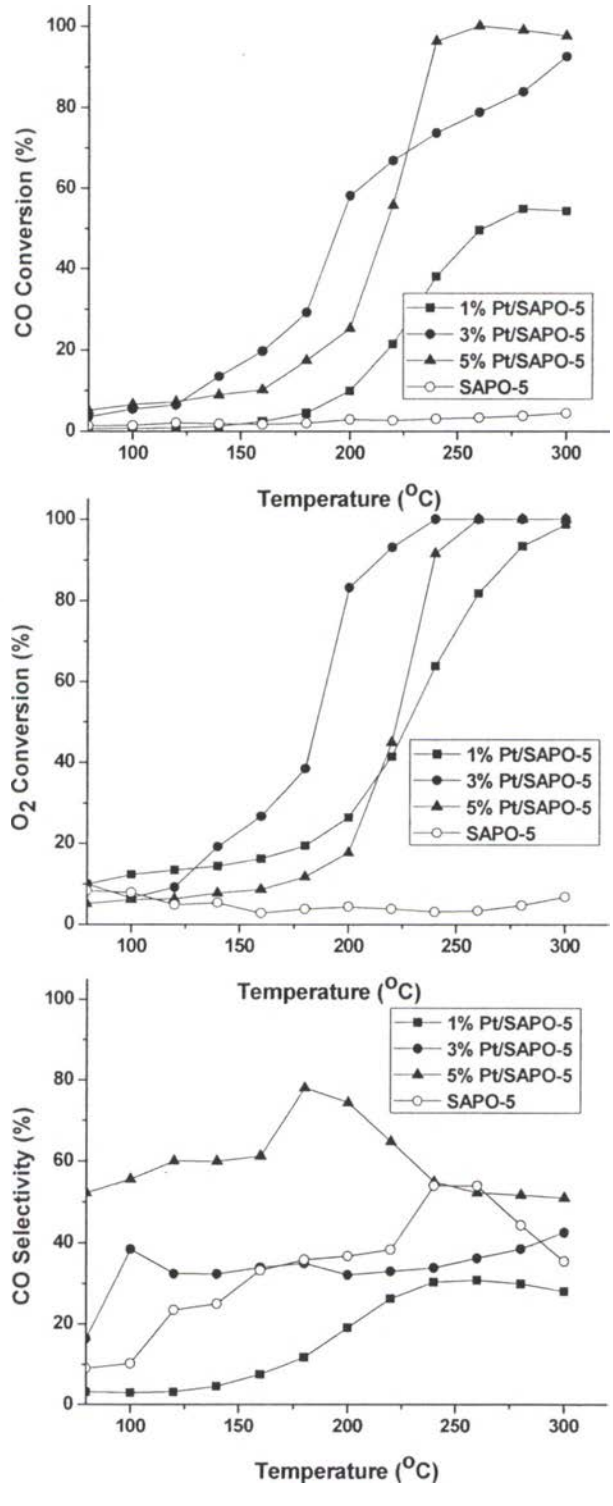

Figure 7.7 CO Conversion (%), O_2 Conversion (%), and CO Selectivity (%) of Pt impregnated SAPO-5 prepared using atrane precursors at various % w/w Pt contents.

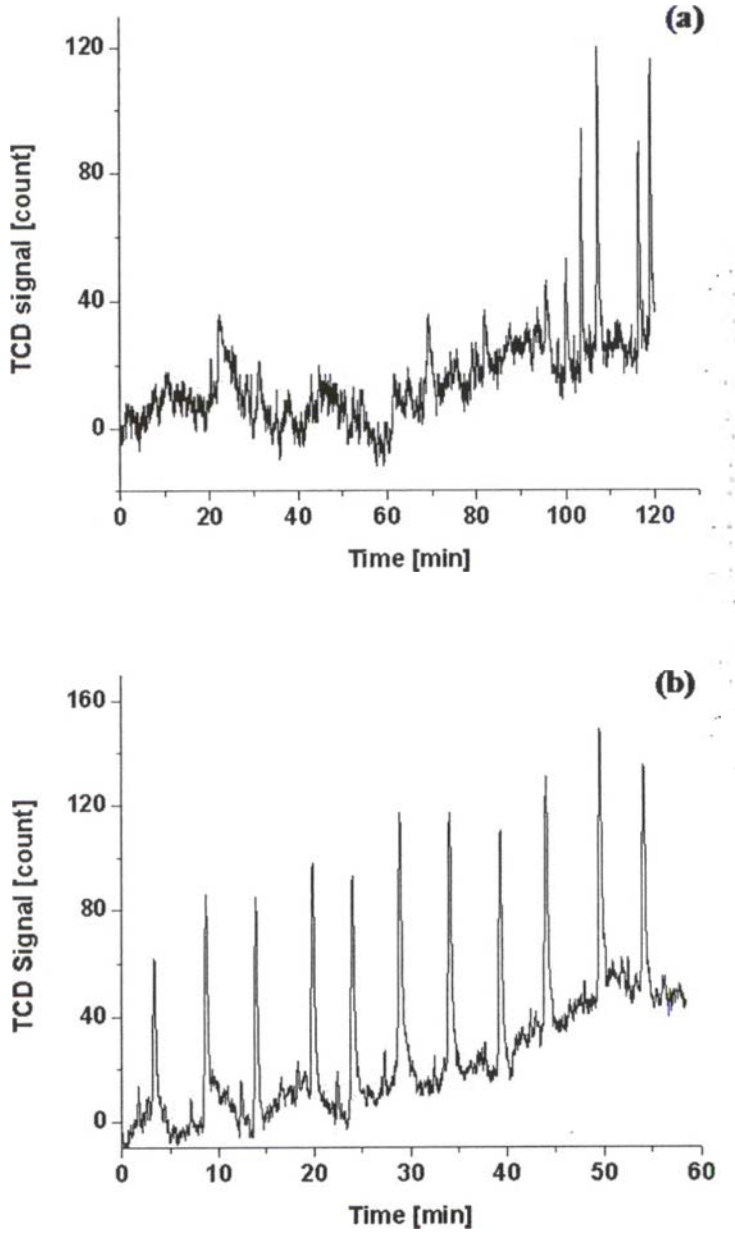

Figure 7.8 CO chemisorption isotherms of (a) 3% Pt/mesoporous $AlPO_4$-5, and (b) 3% Pt/mesoporous SAPO-5

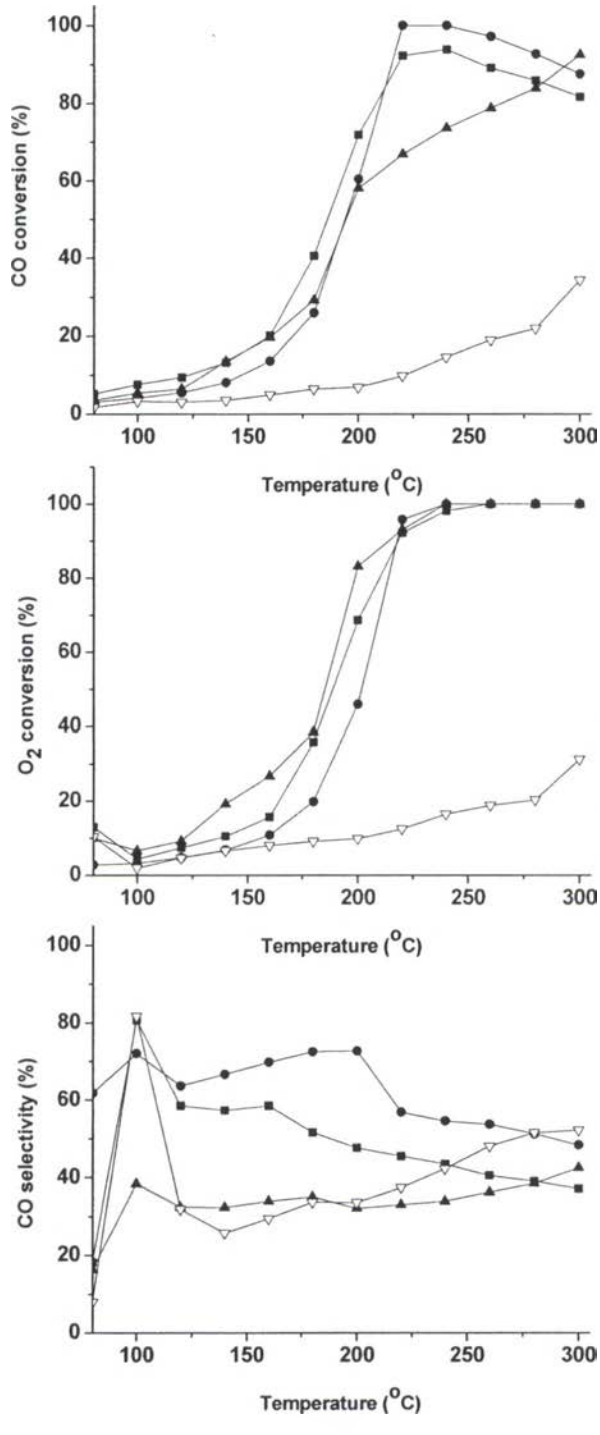

Figure 7.9 CO Conversion (%), O_2 Conversion (%), and CO Selectivity (%) of Pt impregnated on $AlPO_4$-5 (—●—) and SAPO-5 (—▲—) using atrane precursors, Pt impregnated on $AlPO_4$-5 using aluminum isopropoxide precursor (—■—), and Pt loaded via the sol-gel process on $AlPO_4$-5 using atrane precursor (—▽—) at 3% w/w Pt content.

Table 7.1 BET surface area of catalysts before and after Pt loading.

Sample	BET surface area	
	Before Pt loading	After Pt loading
[a]Mesoporous $AlPO_4$-5	170	88
[a]Mesoporous SAPO-5	227	131
[b]Conventional $AlPO_4$-5	113	66
[a]Pt$AlPO_4$-5	-	87

[a]Sample prepared using atrane precursor.

[b]Sample prepared using aluminum isopropoxide precursor.